COMPARATIVE ANALYSIS OF MECHANICAL PROPERTIES AND MICROSTRUCTURE OF COARSE-GRAINED AND NANOSTRUCTURED NONEQUIATOMIC MEDIUM-ENTROPY ALLOYS $Fe_{40}Mn_{40}Co_{10}Cr_{10}$ AND $Fe_{50}Mn_{30}Co_{10}Cr_{10}$ IN THE TEMPERATURE RANGE OF 4.2–300 K

S. E. Shumilin[1], T. V. Hryhorova[1], S. N. Smirnov[1], Yu. O. Semerenko[1], I. V. Kashuba[1], Yu. O. Shapovalov[1], E. D. Tabachnikova[1], M. A. Tikhonovsky[2], Y. Huang[3], T. G. Langdon[4]

[1]B.Verkin Institute for Low Temperature Physics and Engineering of NAS of Ukraine,47 Nauky Ave., Kharkiv, 61103, Ukraine

[2]National Science Center "Kharkiv Institute of Physics and Technology" of NAS of Ukraine, 1 Akademichna Str., Kharkiv, 61108, Ukraine

[3]Department of Design and Engineering, Faculty of Science and Technology, Bournemouth University, Poole, Dorset BH12 5BB, UK

[4]Materials Research Group, Department of Mechanical Engineering, University of Southampton, Southampton SO17 IBJ, UK

E-mail: grigorova@ilt.kharkov.ua

In this work significant differences in the microhardness values and microstructure characteristics were established in nonequiatomic medium-entropy alloys (MEA) Fe40Mn40Co10Cr10 (TWIP) and Fe50Mn30Co10Cr10 (TRIP) in the coarse-grained (CG) and nanostructured (NS) states.

Subject - CG и NS MEA alloys $Fe_{40}Mn_{40}Co_{10}Cr_{10}$ (TWIP) и $Fe_{50}Mn_{30}Co_{10}Cr_{10}$ (TRIP).

Research methods - X-ray diffraction analysis, transmission electron microscope studies, the Vickers microhardness measurements, uniaxial compression testing of 300 – 4.2 K with a strain rate of 3×10^{-4} s^{-1} (yield strength $\sigma_{0.2}$, ultimate strength σ_U, ultimate strain ε_U or ε_{max}), dynamic Young's modulus. High-pressure torsion (HPT) deformation at the two temperatures of 300 K and 77 K.

Microstructure of the TWIP and TRIP alloy in different structural states.

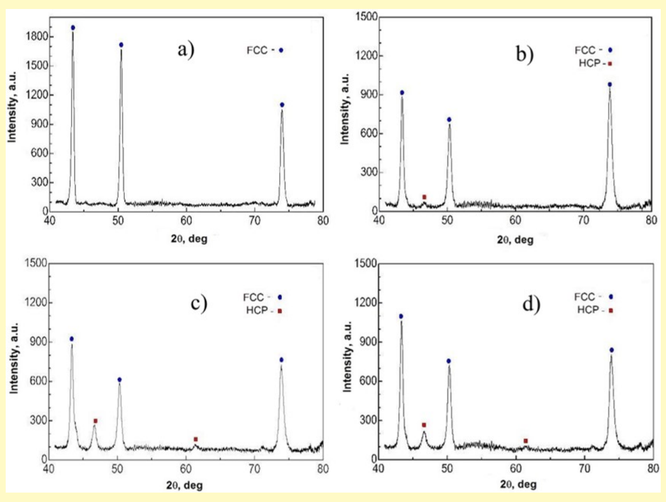

Diffraction patterns of the structure of CG TWIP alloy in different structural states: initial (a); deformed by tension to fracture at temperatures: T = 295 K (b), T = 77 K (c), T = 4.2 K (d).

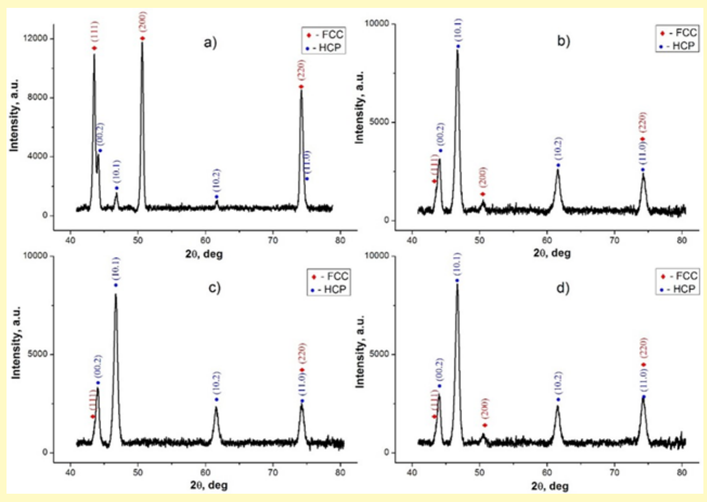

Diffraction patterns of the CG TRIP alloy in different structural states: initial (a); deformed by tension to fracture at temperatures: T = 295 K (b), T = 77 K (c), T = 4.2 K (d).

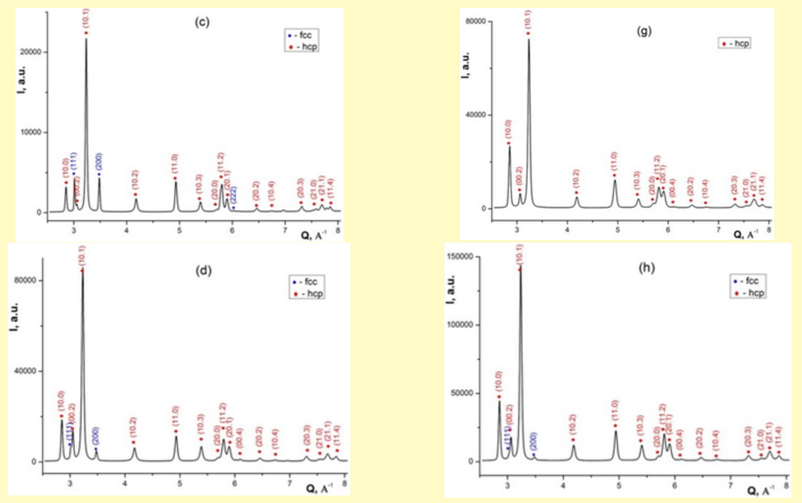

Diffraction patterns at γ = 175. For the NS TWIP alloy: (c) – HPT 300 K, (d) – HPT 77 K. For the NS TRIP alloy: (g) – HPT 300 K, (h) – HPT 77 K.

Phase composition and microhardness for initial (CG) and NS TWIP and TRIP alloys, after HPT for the number of revolutions n = 0.25 and n = 5.

γ – shear strain after HPT, Hv – Vickers microhardness, D – crystallite size, <ε> – microstrain, tfp – twin faults probability, n – number of revolutions at HPT.

Sample	*n*	γ	Temperature HPT, K	Phase	Fraction, vol %	Lattice parameters, Å	Microstructural parameters			Hv GPa
							D, nm	10^3< ε>	10^3 tfp	
TWIP initial	0	0		hcp	0					
				fcc	100	3.624				1.31
TRIP initial	0	0		hcp	41.0	*a* = 2.542, *c* = 4.104				2.48
				fcc	59.0	3.604	215.0	< 0.5		
TWIP-HPT	0.25	8.84	300	hcp	83.4	*a* = 2.546, *c* = 4.114	48.	2.24	4.1	4.15
				fcc	16.6	3.608	87.2	1.95		
			77	hcp	95.9	*a* = 2.546, *c* = 4.113	42.4	3.4	6.9	4.26
				fcc	4.1	3.611	–	–		
	5	177	300	hcp	81.8	*a* = 2.546, *c* = 4.113	54.0	2.24	4.3	4.78
				fcc	18.2	3.609	74.7	1.66		
			77	hcp	93.9	*a* = 2.547, *c* = 4.122	42.4	2.96	6.8	5.41
				fcc	6.1	3.613	34.1	1.64		
TRIP-HPT	0.25	8.84	300	hcp	89.7	*a* = 2.544, *c* = 4.103	53.5	2.99	5.2	4.37
				fcc	10.3	3.601	42.6	1.78		
			77	hcp	96.5	*a* = 2.543, *c* = 4.099	44.2	3.64	6.4	4.85
				fcc	3.5	3.598	–	–		
	5	177	300	hcp	100	*a* = 2.543, *c* = 4.106	42.7	4.03	4.1	5.15
				fcc	0	–	–	–		
			77	hcp	98.5	*a* = 2.543, *c* = 4.106	59.6	3.45	5.4	5.59
				fcc	1.5	3.605	–	–	–	

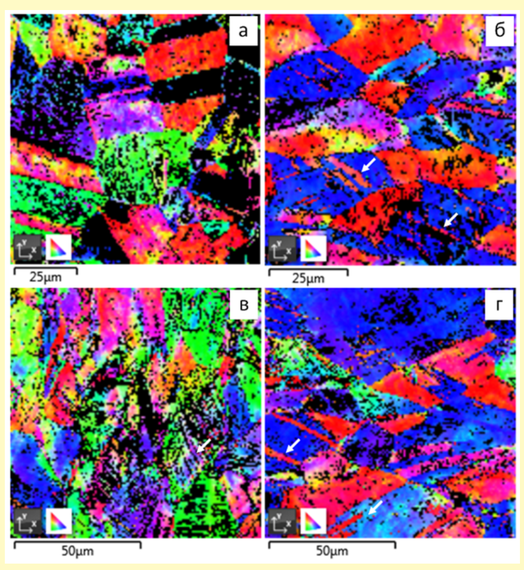

Electron diffraction (EBSD) images of the microstructure of the CG TWIP alloy in different structural states: (a) - initial state; deformed to failure at different temperatures: (b) - T = 295 K, (c) - T = 77 K, (d) - T = 4.2 K. Orientation map in the colors of the inverse pole figures (OPF). Twins are indicated by white arrows.

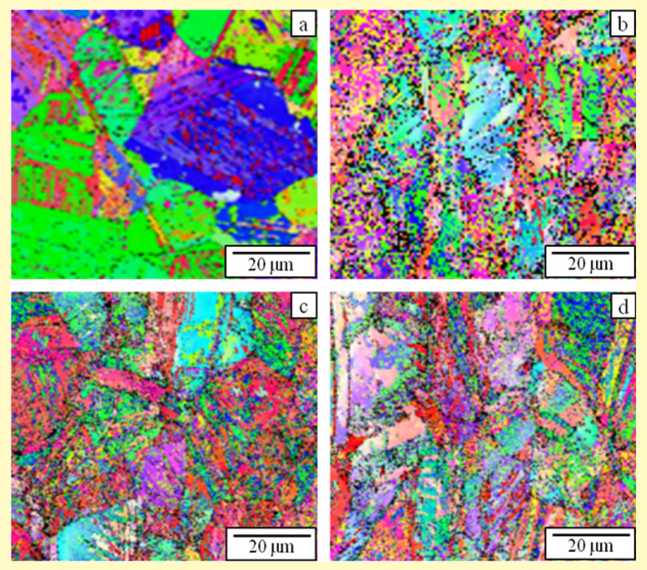

EBSD maps of the CG TRIP of the IPF characterization of the evolution of microstructure before deformation (a) and deformed to fracture for T = 295 K (b), T = 77 K (c), T = 4.2 K (d).

Cryogenic plasticity characteristics of the CG TWIP alloy.

T, K	$\sigma_{0.2}$, МПа	σ_U, МПа	ε_U
295	191	746	0,46
150	324	1452	0,5
77	414	1710	0,46
30	550	-	-
4,2	579	1805	0,456
0,5	543	1690	0,43

Cryogenic plasticity characteristics of the CG TRIP alloy.

T, K	Yield strength $\sigma_{0.2}$, MPa	Ultimate strength σ_U, MPa	Uniform elongation ε, %
295	230	758	50
77	450	1384	48
30	586	1452	47
4,2	606	1513	47
0,5	536	1274	54

Cryogenic plasticity characteristics of the TWIP alloy in the NS state tested under uniaxial compression, and in an initial state.

Sample	Compression temperature, K	$\sigma_{0.2}$, GPa	ε_{max}, %	σ_U, GPa
Initial	300	0.19	46	0.75
	77	0.41	46	1.71
RT-HTP	300	1.49	5.38	1.82
	77	1.97	5.15	2.32
cryo-HPT	300	1.62	6.62	1.84
	77	2.17	3.5	2.38

Acoustic properties.

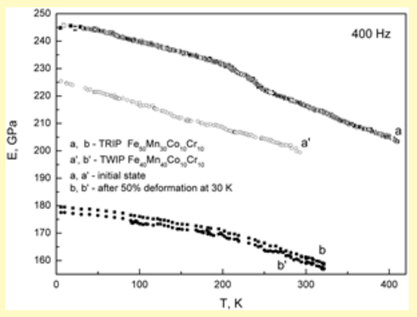

Temperature dependences of the dynamic Young's modulus both in the initial (a - TRIP; b - TWIP) and in the deformed state (a' - TRIP; b' - TWIP).

Summary and conclusions

Comprehensive experimental studies of the microstructure, low-temperature plastic deformation and acoustic properties of medium-entropy nonequiatomic TWIP and TRIP alloys $Fe_{50}Mn_{30}Co_{10}Cr10$ and $Fe_{40}Mn_{40}Co_{10}Cr_{10}$ in CG and NS states were carried out.

1. In TWIP and TRIP alloys, a thermally activated nature of plastic deformation is observed both in the CG and NS states.
2. The single-phase fcc structure of the undeformed TWIP alloy under compression deformation to failure, due to the activation of twinning processes, promotes the fcc-hcp transformation, which is significantly enhanced by decreasing the deformation temperature from 300 K to 4.2 K.
   The two-phase structure (59% fcc and 41% hcp) of the undeformed TRIP alloy during compression deformation to failure, due to the activation of additional fcc-hcp phase transformations, transforms into a practically single-phase hcp structure (about 97% hcp), regardless of the deformation temperature in the range of 4.2-300 K.
3. As results of HPT deformation, in the NS TWIP and NS TRIP alloys, a basically complete phase transition from the fcc phase to hcp phase is observed, the content of which does not depend very strongly on the temperature and the number of revolutions in HPT.
4. HPT deformation leads to a significant reduction in differences in phase composition and in the microhardness values for TWIP and TRIP alloys observed in the coarse-grained state.
5. HPT deformation leads to a significant increase in the microhardness Hv, and in the TWIP alloy this effect is more pronounced than in the TRIP alloy. Reducing the HPT temperature from 300 K to 77 K results in an increase in the Hv value in TWIP and TRIP alloys.
6. It was found that the microstructure of the CG and NS samples of TWIP and TRIP F alloys remains stable over a long period of time.
7. It has been established that the NS TWIP alloy remains ductile under active compression deformation at 300 K and 77 K, while there is no macroscopic plasticity in the NS TRIP alloy under similar conditions.
8. Deformation of 50% at 30 K both TRIP and TWIP alloys leads to a significant reduction in the absolute values of the modulus in the entire temperature range studied. It can be associated with changes in the microstructure of the alloys due to the growth of the HCP phase induced by deformation.